

hep-ph/9910440

Electromagnetic Signals of Hot Hadronic Matter ¹Jan-e Alam^{a,2}, Sourav Sarkar^b, Pradip Roy^c, T. Hatsuda^a
and Bikash Sinha^{b,c}*a) Physics Department, Kyoto University, Kitashirakawa, Kyoto 606-8502, Japan**b) Variable Energy Cyclotron Centre, 1/AF Bidhan Nagar, Calcutta 700 064 India**c) Saha Institute of Nuclear Physics, 1/AF Bidhan Nagar, Calcutta 700 064 India***Abstract**

The photon and dilepton emission rates from quark gluon plasma and hot hadronic matter have been evaluated. The in-medium modifications of the particles appearing in the internal loop of the self energy diagram are taken into account by using a phenomenological effective Lagrangian approach, Brown-Rho and Nambu scaling scenarios. We note that the in-medium effects on the low invariant mass distribution of dilepton and transverse momentum spectra of photon are clearly visible.

I. Introduction

Numerical simulations of the QCD (Quantum Chromodynamics) equation of state on the lattice predict that at very high density and/or temperature hadronic matter undergoes a phase transition to Quark Gluon Plasma (QGP) [1]. One expects that ultrarelativistic heavy ion collisions (URHIC) might create conditions conducive for the formation and study of QGP. Various model calculations have been performed to look for observable signatures of this state of matter. However, among various signatures of QGP, photons and dileptons are known to be advantageous, primarily so because, electromagnetic interaction could lead to detectable signal. However, it is weak

¹Based on talk given by J.A. in the National Seminar on Nuclear Physics, July 26-29, 1999, Institute of Physics, Bhubaneswar, India.

²On leave from Variable Energy Cyclotron Centre, 1/AF Bidhan Nagar, Calcutta 700 064, India

enough to let the produced particles (real photons and dileptons) escape the system without further interaction and thus carrying the information of the constituents and their momentum distribution in the thermal bath.

The disadvantage with photons is the substantial background from various processes (thermal and non-thermal) [2]. Among these, the contribution from hard QCD processes is well understood in the framework of perturbative QCD and the yield from hadronic decays e. g. $\pi^0 \rightarrow \gamma\gamma$ can be accounted for by invariant mass analysis. However, photons from the thermalized hadronic gas pose a more difficult task to disentangle. Therefore it is very important to estimate photons from hot and dense hadronic gas along with the possible modifications of the hadronic properties.

We organize the paper as follows. In section II we discuss the specific reactions which are used to calculate the photon and dilepton emission rate from a thermal bath. In section III we discuss the medium modifications of hadrons. Section IV is devoted for evolution dynamics. Results are presented in section V.

II. Photon and Dilepton Emission Rates

The basic aim of URHIC is to distinguish between the following two possibilities:

$$\begin{aligned} \mathbf{A} + \mathbf{A} \rightarrow \mathbf{QGP} \rightarrow \mathbf{Mixed\ Phase} \rightarrow \mathbf{Hadronic\ Phase} \\ \text{or} \\ \mathbf{A} + \mathbf{A} \rightarrow \mathbf{Hadronic\ Phase} \end{aligned}$$

The former (latter) case where the initial state is formed in QGP (hadronic) phase will be called the ‘QGP scenario’ (‘no phase transition scenario’). In the present work we will contrast the photon and dilepton spectra originating from these two scenarios for SPS and RHIC energies.

The thermal emission rate of a real photon of energy E and momentum p can be expressed in terms of the trace of the retarded photon self energy ($\Pi_{\mu\nu}^R$) at finite temperature [3, 4]

$$E \frac{dR}{d^3p} = -\frac{2}{(2\pi)^3} \text{Im} \Pi_{\mu}^{\mu R}(p) \frac{1}{e^{E/T} - 1} \quad (1)$$

where T is the temperature of the thermal medium. The emission rate of thermal dileptons (virtual photon) differs from that of real photon (due to

different phase space factor) in the following way,

$$\frac{dR}{d^4q} = \frac{\alpha}{12\pi^4 q^2} \left(1 + \frac{2m^2}{q^2}\right) \sqrt{1 - \frac{4m^2}{q^2}} \text{Im}\Pi_\mu^{R\mu} \frac{1}{e^{q_0/T} - 1} \quad (2)$$

The photon emission rate due to Compton and annihilation processes in QGP was performed in Refs. [5, 6] by applying the Hard Thermal Loop (HTL) resummation [7, 8]. The rate of hard photon ($E > T$) emission due to these processes is given by [5]

$$E \frac{dR_\gamma^{QGP}}{d^3q} = \frac{5}{9} \frac{\alpha\alpha_s}{2\pi^2} T^2 e^{-E/T} \ln(2.912E/g^2T). \quad (3)$$

Recently, the bremsstrahlung contribution to photon emission rate has been computed [9] by evaluating the photon self energy in two loop HTL approximation. The physical processes arising from two loop contribution are the bremsstrahlung of quarks, antiquarks and quark anti-quark annihilation with scattering in the thermal bath. The rate of photon production due to bremsstrahlung process for a two flavor thermal system with $E > T$ is given by [9]

$$E \frac{dR_\gamma^{QGP}}{d^3q} = \frac{40}{9\pi^5} \alpha\alpha_s T^2 e^{-E/T} (J_T - J_L) \ln 2, \quad (4)$$

and the rate due to $q - \bar{q}$ annihilation with scattering in the thermal bath is given by,

$$E \frac{dR_\gamma^{QGP}}{d^3q} = \frac{40}{27\pi^5} \alpha\alpha_s ET e^{-E/T} (J_T - J_L), \quad (5)$$

where $J_T \approx 4.45$ and $J_L \approx -4.26$. The most important implication of this work is that the two loop contribution is of the same order of magnitude as those evaluated at one loop [5, 6] due to the larger size of the available phase space. The net rate of emission is obtained by adding eqs. 3, 4 and 5.

In the hadronic matter (HM) an exhaustive set of hadronic reactions and vector meson decays involving π , ρ , ω and η mesons have been considered. It is well known [5] that the reactions $\pi\rho \rightarrow \pi\gamma$, $\pi\pi \rightarrow \rho\gamma$, $\pi\pi \rightarrow \eta\gamma$, $\pi\eta \rightarrow \pi\gamma$, and the decays $\rho \rightarrow \pi\pi\gamma$ and $\omega \rightarrow \pi\gamma$ are the most important channels for photon production from hadronic matter in the energy regime of our interest. The rates for these processes could be evaluated from the imaginary part of the two loop photon self energy involving various mesons.

The photon emission rate from $\pi \rho \rightarrow \pi \gamma$ via the intermediary a_1 has also been included.

We have considered quark anti-quark annihilation for the evaluation of dilepton emission rate from QGP, which is given by

$$\frac{dR}{dM} = \frac{\sigma_{q\bar{q}}(M)}{(2\pi)^4} M^4 T \sum_n \frac{K_1(nM/T)}{n} \quad (6)$$

with the cross section

$$\sigma_{q\bar{q} \rightarrow e^+e^-} = \frac{80\pi}{9} \frac{\alpha^2}{M^2} \sqrt{\left(1 - \frac{4m^2}{M^2}\right)} \left(1 + \frac{2m^2}{M^2}\right). \quad (7)$$

For low mass dilepton emission rate we consider the yield from $\pi^+\pi^- \rightarrow e^+e^-$, $\rho \rightarrow e^+e^-$ and $\omega \rightarrow e^+e^-$ (see [10, 11] for details).

III. Medium Effects

To study the medium effects on the transverse momentum distribution of photons and invariant mass distribution of dileptons from URHIC we need two more ingredients. Firstly, we require the variation of masses and decay widths with temperature, because the invariant matrix element for photon (real and virtual) production suffer in-medium modifications through the temperature dependent masses and widths of the participants. As the hadronic masses and decay widths enter directly in the count rates of electromagnetically interacting particles, the finite temperature effects in the cross sections, particularly in the hadronic matter are very important in URHIC.

We consider the following scenarios for the in-medium vector meson mass variations in the present work.

(I) Walecka Model [12]

We have evaluated the in-medium mass of ρ and ω mesons and decay widths within the framework of Walecka model. The renormalization procedure of Refs. [13, 14] has been used to render the vacuum self energy of vector mesons finite. The details of the calculations at non-zero T can be found in our previous works [10, 11, 15, 16, 17] and we do not reproduce them here. However, from the results of those calculations the variation of nucleon, rho and omega masses and the decay width(Γ_ρ) of rho with temperature at zero baryon density can be parametrized as (see also [18])

$$m_N^*/m_N = 1 - 0.0264x^{8.94}, \quad m_\rho^*/m_\rho = 1 - 0.1268x^{5.24} \quad (8)$$

$$m_\omega^*/m_\omega = 1 - 0.0438x^{7.09}, \quad \Gamma_\rho^*/\Gamma_\rho = 1 + 0.664x^4 - 0.625x^5 \quad (9)$$

where asterisk indicates effective mass/width in the medium, $x = T/T_c$ and $T_c = 0.16$ GeV. According to our calculation the nucleon, rho and omega masses decrease differently.

(II) Brown-Rho and Nambu Scaling [19, 20]

In the previous it is mentioned that both the photon and dilepton emission rates are proportional to imaginary part of the current-current correlation functions (spectral function). We have parameterized the hadronic spectral functions with a conspicuous resonance plus a continuum. These spectral functions (in vacuum) for the isovector and isoscalar channel have been constrained from experimental data on $e^+e^- \rightarrow \text{hadrons}$. At finite temperature we have parameterized the vector meson mass (pole) and the continuum threshold (ω_0) of the spectral function as a function of temperature in the following way (see Ref. [17] for details):

$$\frac{m_V^*}{m_V} = \frac{\omega_0^*}{\omega_0} = \left(1 - \frac{T^2}{T_c^2}\right)^\lambda, \quad (10)$$

where λ is a sort of *dynamical* critical exponent and V stands for vector mesons (ρ and ω). Since the numerical value of λ is not known, we take two typical cases: $\lambda = 1/6$ (BR scaling) and $1/2$ (Nambu scaling) [20].

IV. Evolution Dynamics

The observed photon spectrum originating from an expanding QGP or hadronic matter is obtained by convoluting the static (fixed temperature) rate, as given by Eqs. (1) and (2), with expansion dynamics. Therefore, the second ingredient required for our calculations is the description of the system undergoing rapid expansion from its initial formation stage to the final freeze-out stage. In this work we use Bjorken-like [21] hydrodynamical model for the isentropic expansion of the matter in $(1+1)$ dimension. For the QGP sector we use a simple bag model equation of state (EOS) with two flavor degrees of freedom. The temperature in the QGP phase evolves according to Bjorken scaling law $T^3 \tau = T_i^3 \tau_i$. In the hadronic phase we have to be more careful about the presence of heavier particles and their change in masses due to finite temperature effects. The hadronic phase consists of π , ρ , ω , η and a_1 mesons and nucleons. The nucleons and heavier mesons may play an important role in the EOS in a scenario where mass of the

hadrons decreases with temperature. The energy density and pressure for such a system of mesons and nucleons is given by,

$$\epsilon_H = \sum_{i=\text{mesons}} \frac{g_i}{(2\pi)^3} \int d^3p E_i f_{BE}(E_i, T) + \frac{g_N}{(2\pi)^3} \int d^3p E_N f_{FD}(E_N, T) \quad (11)$$

and

$$P_H = \sum_{i=\text{mesons}} \frac{g_i}{(2\pi)^3} \int d^3p \frac{p^2}{3E_i} f_{BE}(E_i, T) + \frac{g_N}{(2\pi)^3} \int d^3p \frac{p^2}{3E_N} f_{FD}(E_N, T) \quad (12)$$

where the sum is over all the mesons under consideration and N stands for nucleons and $E_i = \sqrt{p^2 + m_i^2}$. The entropy density is given by

$$s_H = \frac{\epsilon_H + P_H}{T} \equiv 4a_{\text{eff}}(T) T^3 = 4 \frac{\pi^2}{90} g_{\text{eff}}(m^*(T), T) T^3 \quad (13)$$

where g_{eff} is the effective statistical degeneracy.

Thus, we can visualize the effect of finite mass of the hadrons through an effective degeneracy $g_{\text{eff}}(m^*(T), T)$ of the hadronic gas. The variation of temperature from its initial value T_i to final value T_f (freeze-out temperature) with proper time (τ) is governed by the conservation of entropy

$$s\tau = s_i\tau_i \quad (14)$$

The initial temperature of the system is obtained by solving the following equation self consistently

$$\frac{dN_\pi}{dy} = \frac{45\zeta(3)}{2\pi^4} \pi R_A^2 4a_{\text{eff}} T_i^3 \tau_i \quad (15)$$

where dN_π/dy is the total pion multiplicity, R_A is the radius of the system, τ_i is the initial thermalization time and $a_{\text{eff}} = (\pi^2/90) g_{\text{eff}}$. The change in the expansion dynamics as well as the value of the initial temperature due to medium effects enters the calculation of the photon and dilepton emission rates through the effective statistical degeneracy.

V. Results and Discussions

Having obtained the finite temperature effects on hadronic properties and the cooling laws we now integrate the rates obtained in the previous sections

over the space-time evolution of the collision. We must account for the fact that the thermal rates are evaluated in the rest frame of the emitting matter and hence the momenta of the emitted photons or dileptons are expressed in that frame. Accordingly, the integral over the expanding matter is of the form

$$\frac{dN}{d\Gamma} = \int_{\text{formation}}^{\text{freeze-out}} d^4x \frac{dR(E^*, T(x))}{d\Gamma} \quad (16)$$

where $d\Gamma$ stands for invariant phase space elements: d^3p/E for photons and d^4q for dileptons. E^* is the energy of the photon or lepton pair in the rest frame of the emitting matter and $T(x)$ is the local temperature. In a fixed frame like the laboratory or the centre of mass frame, where the 4-momentum of the photon or lepton pair is $q_\mu = (E, \vec{q})$ and the emitting matter element d^3x moves with a velocity $u_\mu = \gamma(1, \vec{v})$, the energy in the rest frame of the fluid element is given by $E^* = u_\mu q^\mu$.

As discussed earlier, g_{eff} is obtained as a function of T by solving Eq.(13). A smaller (larger) value of g_{eff} is obtained in the free (effective) mass scenario. As a result we get a larger (smaller) initial temperature by solving Eq.(15) in the free (dropping) mass scenario for a given multiplicity. Naively we expect that at a given temperature if a meson mass drops its Boltzmann factor will be enhanced and more of those mesons will be produced leading to more photons [15]. However, a larger drop in the hadronic masses results in smaller initial temperature, implying that the space time integrated spectra crucially depends on these two competitive factors. Therefore, with (without) medium effects one integrates an enhanced (depleted) static rate over smaller (larger) temperature range for a fixed freeze-out temperature ($T_f = 130$ MeV in the present case). In the present calculation (Fig. (1) for Pb+Pb collisions at SPS energies, $dN/dy = 600$) the enhancement in the photon emission due to the higher initial temperature in the free mass scenario (where static rate is smaller) overwhelms the enhancement of the rate due to negative shift in the vector meson masses (where the initial temperature is smaller). Accordingly, in the case of bare mass (Nambu scaling) scenario the photon yield is the highest (lowest). In case of the Walecka model, the photon yield lies between the above two limits.

In the ‘QGP scenario’ the photon yield with in-medium mass is lower than the case where bare masses of hadrons are considered. However, the difference is considerably less than the ‘no phase transition scenario’. This is because, in this case the initial temperature is determined by the quark

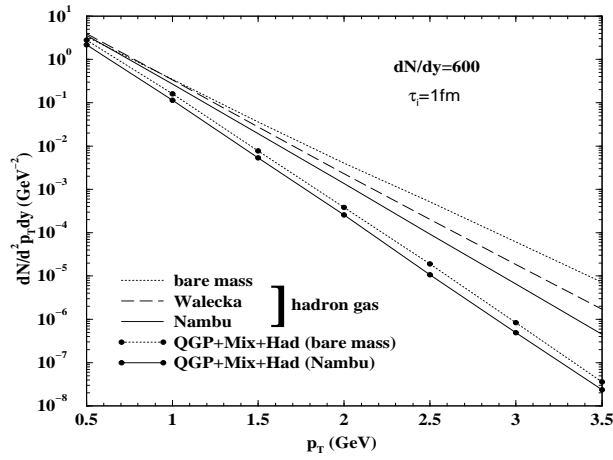


Figure 1: Total thermal photon yield corresponding to $dN/dy = 600$ and $\tau_i = 1$ fm/c. The solid (long-dash) line indicates photon spectra when hadronic matter formed in the initial state at $T_i = 195$ MeV ($T_i = 220$ MeV) and the medium effects are taken from Nambu scaling (Walecka model). The dotted line represents the photon spectra without medium effects with $T_i = 270$ MeV. The solid (dotted) line with solid dots represent the yield for the ‘QGP scenario’ when the hadronic mass variations are taken from Nambu scaling (free mass).

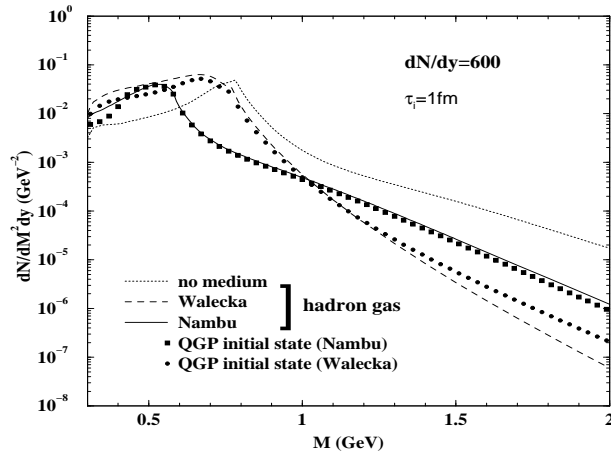


Figure 2: Total thermal dilepton yield corresponding to $dN/dy = 600$ and $\tau_i = 1 \text{ fm/c}$. The solid (long-dash) line indicates dilepton spectra when hadronic matter formed in the initial state at $T_i = 195 \text{ MeV}$ ($T_i = 220 \text{ MeV}$) and the medium effects are taken from Nambu scaling (Walecka model). The dotted line represents the spectra without medium effects with $T_i = 270 \text{ MeV}$. The square (solid dots) line with solid dots represent the yield for the ‘QGP scenario’ when the hadronic mass variations are taken from Nambu scaling (Walecka model).

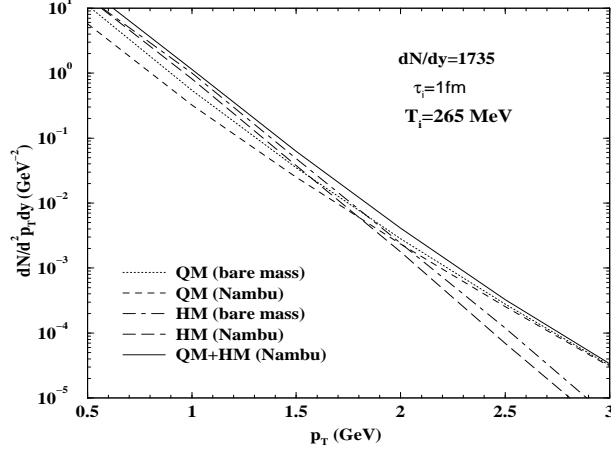


Figure 3: Thermal photon spectra at RHIC energies.

and gluon degrees of freedom and the only difference between the two is due to the different lifetimes of the mixed phase. In Fig. (1), the photon spectra from ‘QGP scenario’ is compared with that from ‘no phase transition scenario’; the latter overshines the former.

The space time integrated dilepton spectra for the ‘QGP scenario’ and ‘no phase transition scenario’ with different mass variation are shown in Fig.(2). The shifts in the invariant mass distribution of the spectra due to the reduction in the hadronic masses according to different models are distinctly visible. Similar to the photon spectra, the dilepton spectra from ‘no phase transition scenario’ dominates over the ‘QGP’ scenario for invariant mass beyond ρ peak.

For RHIC energies, we consider the ‘QGP’ scenario only as a scenario of pure hot hadronic initial state within the format of the model used here appears to be unrealistic. The thermal photon yield for RHIC ($dN/dy = 1735$) is displayed in Fig. (3). The solid line represents the total thermal photon yield originating from initial QGP state, mixed phase and the pure hadronic phase. The short dash line indicates photons from quark matter (QM) (= pure QGP phase + QGP part of the mixed phase) and the long dash line represents photons from hadronic matter (HM) (= hadronic part of the mixed phase + pure hadronic phase). In all these cases the effective masses of the hadrons have been taken from Nambu scaling. For $p_T > 2$ GeV photons from QM overshines those from HM, since most of these high p_T photons originate from the high temperature QGP phase. The dotted

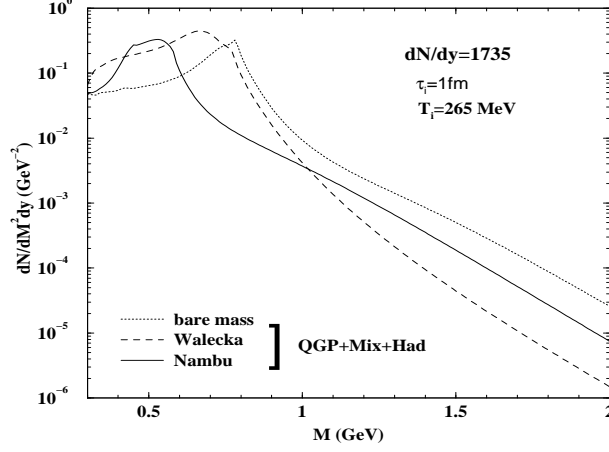


Figure 4: Thermal dilepton spectra at RHIC energies.

and the dotdash lines indicate photon yields from QM and HM respectively with bare masses in the hadronic sector. The HM contribution for the bare mass is larger than the effective mass (Nambu) scenario because of the larger value of the life time of the mixed phase in the earlier case. It is important to note that for $p_T > 2$ GeV, the difference in the QM and HM contribution in the effective mass scenario is more than the bare mass scenario.

Thermal dilepton yield at RHIC energies for QGP initial state and for different mass variation scenarios are shown in Fig. (4). The shape of the peak in the dilepton spectra in case of Walecka model is slightly different(broader) from the other cases because of the larger mass separation between ρ and ω mesons in this case. The dilepton yield beyond the vector meson peak is larger in the bare mass scenario because of the larger life time of the mixed phase.

We have evaluated both the real photon and dilepton emission rate from QGP and hot hadronic matter by taking into accounts in-medium mass modifications of vector mesons according to Walecka Model calculations, BR and Nambu scaling. We observe that the in-medium effects on both photon and dilepton spectra are clearly visible.

Acknowledgement: J. A. is grateful to Japan Society for Promotion of Science (JSPS) for financial support. T. H. was partly supported by Grant-in-Aid for Scientific Research No. 10874042 of the Japanese Ministry of Education, Science, and Culture. J. A. and T. H. were also supported by Grant-in-Aid for Scientific Research No. 98360 of JSPS.

References

- [1] A. Ukawa, Nucl. Phys. **A 638** (1998) 339c.
- [2] J. Alam, S. Raha and B. Sinha, Phys. Rep. **273** (1996) 243.
- [3] L. McLerran and T. Toimela, Phys. Rev. **D31** (1985) 545.
- [4] C. Gale and J. I. Kapusta, Nucl. Phys. **B 357**, (1991) 65.
- [5] J. I. Kapusta, P. Lichard, and D. Seibert, Phys. Rev. **D 44** (1991) 2774.
- [6] R. Baier, H. Nakkagawa, A. Niegawa and K. Redlich, Z. Phys. **C53** (1992) 433.
- [7] E. Braaten and R. D. Pisarski, Nucl. Phys. **B 337** (1990) 569; Nucl. Phys. **B339** (1990) 310.
- [8] J. Frenkel and J. C. Taylor, Nucl. Phys. **B334** (1990) 199.
- [9] P. Aurenche, F. Gelis, H. Zaraket and R. Kobes, Phys. Rev. **D 58** (1998) 085003.
- [10] J. Alam, S. Sarkar, P. Roy, B. Dutta-Roy and B. Sinha, Phys. Rev. **C 59** (1999) 905.
- [11] P. Roy, S. Sarkar, J. Alam, B. Dutta-Roy and B. Sinha, Phys. Rev. **C 59** (1999) 2778.
- [12] B. D. Serot and J. D. Walecka, Advances in Nuclear Physics, Vol. 16, Plenum press, NY 1986.
- [13] H. Shiomi and T. Hatsuda, Phys. Lett. **B334** (1994) 281.
- [14] T. Hatsuda, H. Shiomi and H. Kuwabara, Prog. Th. Phys. **95** (1996) 1009.
- [15] S. Sarkar, J. Alam, P. Roy, A. K. Dutt-Mazumder, B. Dutta-Roy, B. Sinha, Nucl. Phys. **A634**, (1998) 206.
- [16] P. Roy, S. Sarkar, J. Alam and B. Sinha, Nucl. Phys. **A 653** (1999) 277.
- [17] J. Alam, S. Sarkar, P. Roy, T. Hatsuda and B. Sinha, hep-ph/9909267.

- [18] S. Sarkar, P. Roy, J. Alam, and B. Sinha, Phys. Rev. **C** (in press);
nucl-th/9812006.
- [19] G. E. Brown and M. Rho, Phys. Rev. Lett. **66** (1991) 2720.
- [20] G. E. Brown and M. Rho, Phys. Rep. **269** (1996) 333.
- [21] J. D. Bjorken, Phys. Rev. **D27**, (1983) 140.